**SAND2018-11207R**

**LDRD PROJECT NUMBER**: 210569
**LDRD PROJECT TITLE**: Zeptocalorimetry
**PROJECT TEAM MEMBERS**: Tom Harris (1882), Peter Sharma (1867), Tzu-Ming Lu (1867)

## ABSTRACT:

Here we present the development of a Zeptocalorimeter. The motivation for designing and implementing such a device is driven, ultimately, by its anticipated exceptional sensitivity ($10^{-21}$ J/K, at 2K). Such a device would be highly valuable in detecting minute quantities of mass for threat detection, studying fundamental phonon physics, and detecting energetic dissipation events at the attojoule level. To date, the most sensitive calorimeter demonstrated in the literature at 2K has been developed by the Roukes group at Caltech, where they achieved an addendum heat capacity of $10^{-15}$ J/K with a 1/1000 sensitivity to external stimuli. To obtain such a low value of heat capacity requires a very small thermal mass, and thus, one of the greatest challenges in this project is the fabrication of this device, which requires numerous precision nanofabrication techniques. Furthermore, the heat capacity measurement of this device, as performed from room temperature to cryogenic temperatures, is equally challenging, as the transient signals used to determine the platform's thermal time constant require careful attention to the mitigation of feedthrough capacitance and delicate amplifier offsets. In this report we describe in detail the fabrication process flow for developing the calorimeter, including the layout and device design for obtaining a single lumped RC thermal resistance and capacitance, so that the device can be used for quantitative measurements of nanoscale materials with a suitable thermal link. The measurement method and experimental setup are also given, where we explain the heater and thermometer calibration methods, the thermal resistance measurements, the transient measurements, and lastly the cryogenic setup with intermediate frequency cabling and the thermal sinking of those lines.

## INTRODUCTION:

Calorimetry is the measurement of thermal energy either stored or released by a system. These measurements can be performed both qualitatively and quantitatively. In a quantitative sense, calorimetry can be used to determine the temperature-dependent heat capacity of a material, or by integrating the heat capacity as a function of temperature, one can determine the enthalpy of a process. If the mass is known, one may determine the specific heat and/or the specific enthalpy. Common applications of calorimetry involve measuring the heats of reaction (e.g., adsorption, desorption, oxidation, and kinetics), studying phase changes of materials (e.g., vaporization, melting, glass transition, and superconducting transition), and thermal spectroscopy to determine the purity of materials (used in the pharmaceutical industry) or to identify the structure of biomolecules. Typical commercial calorimeters measure bulk samples, operate between 300K to 2K, and may be operated in either single or differential mode.

Sandia National Laboratories is a multimission laboratory managed and operated by National Technology and Engineering Solutions of Sandia, LLC, a wholly owned subsidiary of Honeywell International, Inc., for the U.S. Department of Energy's National Nuclear Security Administration under contract DE-NA-0003525

Microfabricated calorimeters, compared to commercial systems, possess a relatively smaller thermal mass, and because of this drastically reduced size, they inherently have greater sensitivity to thermal signals. Microfabricated calorimeters have been used to make highly sensitive bolometers and transition edge detectors for observing single microwave photons. These devices have been used to study the size effects of thermodynamic properties, including the melting point depression for nanoparticles [1] and the dimensionality of phonons in carbon nanotubes [2]. With regard to electronic solid state systems, the mapping of Fermi surfaces has been performed with microscale calorimetry by studying magnetoscillations in the specific heat using the de Haas – van Alphen effect [3]. Micro and nanoscale fabrication techniques applied to calorimetry devices potentially provide a path forward for studying condensed matter systems rich with physics. For example, Roukes proposed using nanofabrication combined with a gallium arsenide single crystalline structure to perform counting of individual phonons [4].

Throughout the literature three common calorimetry techniques are the most prevalent [5]: (1) the AC Method, (2) the Time Constant Method, and (3) the Adiabatic Relaxation Method. In the AC method, heating at a steady periodic frequency of $2\omega$ with a prescribed power is applied to the system. The temperature response of the system is typically determined from a calibrated thermometer or a mounted temperature sensor, and the quasi-steady response is directly proportional to the thermal mass of the system. The heat capacity is given by the ratio of the heating amplitude and the temperature oscillation, within a constant prefactor. The thermal linkage between the mass and the thermal reservoir is determined by the DC offset in the temperature and the heating amplitude. In the Time Constant method, a heating pulse of known amplitude is applied to the system. Due to the thermal mass of the system and its coupling to the external environment, the system experiences a transient temperature rise and finally settles at a steady-state temperature value. The transient response provides the thermal time constant ($\tau$) of the system and the steady-state response is indicative of the thermal coupling to the environment, $R_{th}$. The heat capacity of the system is then given by the ratio of $\tau$ /$R_{th}$. In the Adiabatic Relaxation method, a heat pulse is also employed, and heat leaks are not quantified, which is why this method is often used in differential scanning calorimetry. For this project, we use the Time Constant method.

## DETAILED DESCRIPTION OF EXPERIMENT/METHOD:

The first formidable challenge in this project was to develop a process flow for manufacturing a calorimeter with a thermal mass small enough to realize a heat capacity sensitivity of $10^{-21}$ J/K at 2K, while maintaining a single lumped thermal resistance and thermal capacitance so that quantitative measurements could be performed on nanomaterials in future experiments. To attain this level of sensitivity, our nanofabricated calorimeter was engineered in a fashion following the work of Fon and Roukes [Refs], where a silicon nitride membrane was formed into a plate tethered by four legs. In this arrangement, the legs form the thermal link to the bath and the central plate comprises the dominant mass and thus the lumped thermal capacitance of the system. Fon showed that a silicon nitride plate with a geometry of 25µm x 25µm x 120nm (square plate widths and thickness, respectively) possessed a heat capacity of $10^{-15}$ J/K at 2K.

Yet this device, coupled with their measurement system, exhibited a measurement sensitivity of $10^{-18}$ J/K at pumped helium temperatures, demonstrated by measuring the heat capacity of a monolayer of helium. Thus, to achieve a $10^{-21}$ J/K level of sensitivity, we pushed the limits of nanofabrication to realize a device that was approximately 1000x smaller than the Fon structure, which in principle should provide the desired level of sensitivity. That is to say, if our calorimetry platform exhibits a heat capacity of $10^{-18}$ J/K at 2K, then if we can attain a 1/1000 measurement sensitivity at this temperature we anticipate reaching the $10^{-21}$ J/K limit. The volume of material used in the Fon platform for their thermal mass equates to $75x10^{-18}$ $m^3$. As the thermal mass scales with volume for equal densities, here, we target a lumped mass with a volume defined by the dimensions 3.5µm x 3.5µm x 10nm (= $1.2x10^{-19}$ $m^3$), which equates to a volume reduction factor of 625 (closely approaching the target value of 1000). For thermal linkages (i.e., the beams) patterned at a width of 50-80nm and at a length of ~1.5µm, the foregoing volume dimensions of the calorimeter plate, compared to the total volume of the legs, constitute a dominant lumped mass for this system with better than 5% error. Assuming that the thermal conductivity of the silicon nitride membrane is determined by the thickness of the membrane, which is uniform, the aforementioned geometry of the thermal linkages, compared to the main calorimeter plate and its approximated thermal resistance, allow the tethers to comprise the dominant thermal resistance of the system, to within 5% error.

To inject heat into the calorimeter and to measure its temperature response, we designed the device with two, independent electrical resistors where one resistor functions as a heater and the other resistor functions as a thermometer. This arrangement, compared to a single heater/thermometer, allows for a separate and independent measurement of the heat traversing the membrane during heating events. To minimize the overall mass of the device, which transcends to the lumped main plate, 4 thermal linkages were used to suspend the plate, where 2 of the linkages were used for the electrical leads to the heater and the other 2 were used for the electrical leads for the thermometer. As a 2-point electrical measurement, for either the heater or the thermometer, both the heater and the thermometer were designed such that each of their electrical resistances was much greater (by 80-90%) than the electrical resistance of the electrical leads patterned along the support legs. In this first-generation design, we relied on resistance thermometry to determine the temperature of the platform.

To perform temperature-dependent measurements on our device, we constructed two cryogenic systems. The first system was a dry, closed-cycle system permitting temperature-dependent measurements from 325K- ~10K. This system was used exclusively to proof-out the device and to develop a general understanding of its performance metrics. To reach temperatures near 1K, we also setup a liquid helium flow cryostat, which permitted the pumping of helium. Both of these systems were outfitted with DC lines and high-frequency coaxially lines permitting a bandwidth of ~10MHz for pulsing measurements.

The second most challenging aspect of this project was the pulsing measurements and the mitigation of feedthrough capacitance through both the device and the device packaging. To measure the thermal resistance of the device, DC heating was applied to the heater and a lock-in amplifier was used on the thermometer to determine the temperature of the platform, after the

thermometer was calibrated. The transient response of the platform was measured using an arbitrary wave form generator outputting a square wave to the heater, with the thermometer's response measured using an oscilloscope.

## RESULTS:

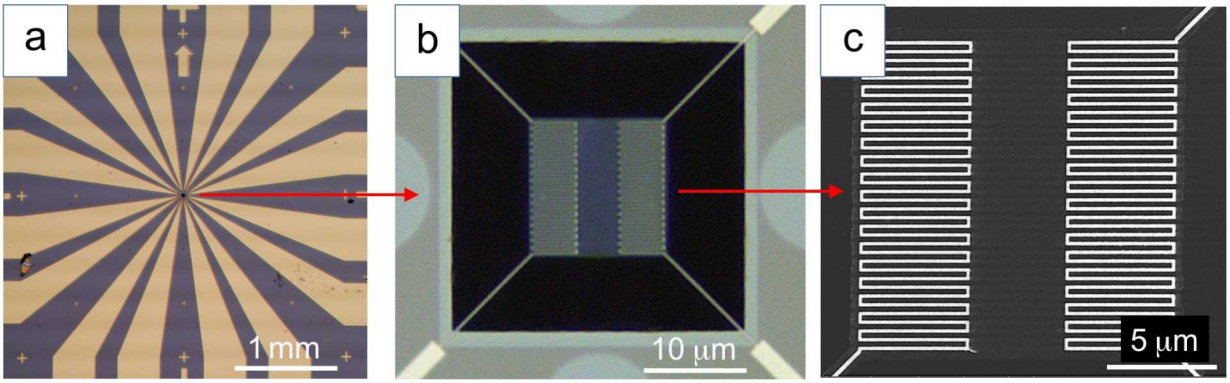


**Fig. 1** The micro/nanofabricated calorimeter. (a) The 5mm x 5mm chip with wire bond pads and electrical leads extending from the center silicon nitride membrane. (b) The center membrane after etching with the suspended calorimeter lumped mass (center) and four tether thermal anchors extending to the thermal bath. (c) The Pt heater and thermometer patterned on the central mass used for injecting heat and sensing the temperature rise of the device.

A major accomplishment in this project was the successful development of a micro/nanofabrication process flow that allowed us to fabricate the calorimeter. Figure 1 shows the completed device. The final device consists of a chip approximately 5mm x 5mm and 400μm thick. We used optical lithography to pattern gold traces that extend from the central region where the calorimeter resides to the edge of the chip where bond pads are located. The calorimeter's main mass plate and the thermal anchors were patterned with electron beam lithography. The device was suspended using a dry etch. Both the heater and the thermometer were patterned using electron beam lithography followed by a platinum evaporation. After the device was fabricated, it was wire-bonded to a ceramic package and mounted into a cryostat for temperature dependent measurements.

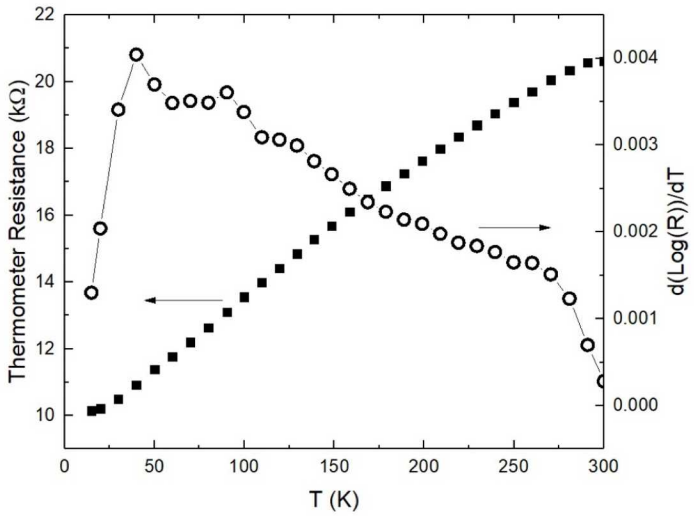


**Fig. 2**. Left scale: thermometer resistance as a function of temperature. Right scale: dLogR/dT of the curve on the left scale. The right scale indicates the fractional change in resistance expected from a 1 K temperature change. This number must be higher to achieve better measurements.

An example thermometer calibration is shown in Fig. 2. The resistance of the Pt thermometer is read using a lock in amplifier. A sinusoidal voltage of about 2 mVrms amplitude is applied to one end of the thermometer. The other end of the thermometer is connected to a DL1211 transimpedance amplifier at a gain of $10^6$. The output of the DL1211 is then connected to the single ended input of the lock in. A time constant of 30 ms was used with a roll off of 24 dB/octave low pass filter to set the bandwidth. In this way, the resistance of both Pt traces were measured as a function of temperature. The temperature was stabilized using a Lakeshore 335 temperature controller. Each Pt trace had a similar resistance versus temperature curve. The sensitivity of the calorimeter depends on the change in resistance of the Pt trace with temperature, quantified by d(log R)/dT, which gives the fractional change in resistance expected for a desired temperature rise. For the data shown in Fig. 2, the temperature coefficient of resistance (right scale) indicates an expected change of about 6 Ohms for a temperature rise of 1 K. This is a difficult signal to measure.

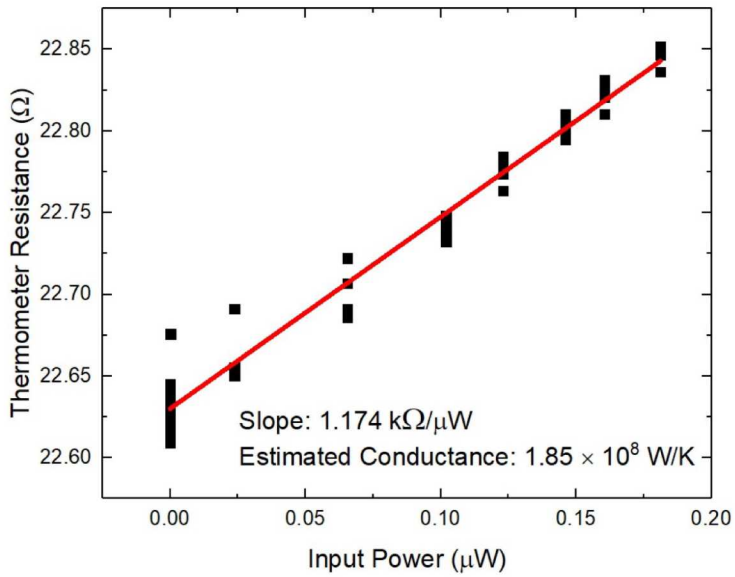


**Fig. 3**. Thermal conductance measurement. The resistance of one Pt trace is read out as the power is increased on the opposite Pt trace. The resistance change, and therefore temperature change, is linear with power, allowing an estimate of the conductance of 1.85e8 W/K, which is 5-10 times the estimated design value.

The second step in the measurement is to estimate the thermal conductance of the platform. This was

accomplished by heating one of the Pt traces with a DC current, sourced using a Keithley 2400 sourcemeter, and measuring the temperature rise on the opposite Pt trace. Either trace can be used as thermometer or heater, as they are symmetric. The temperature rise was measured using a lock in method in the same way as described earlier, with a 1 second time constant. The larger time constant was needed to detect smaller temperature rises. Fig. 3 shows an example of a thermal conductance measurement. The change in resistance is measured as a function of power dissipated on the platform, given by $I^2R$ for the Pt trace designated as the heater. This curve is linear with power, and so a slope can be defined as the thermal conductance. This curve was taken at 290 K, yielding a thermal conductance of 1.85e8 W/K. This estimate for the conductance is larger than the estimated design value by a factor of 5-10.

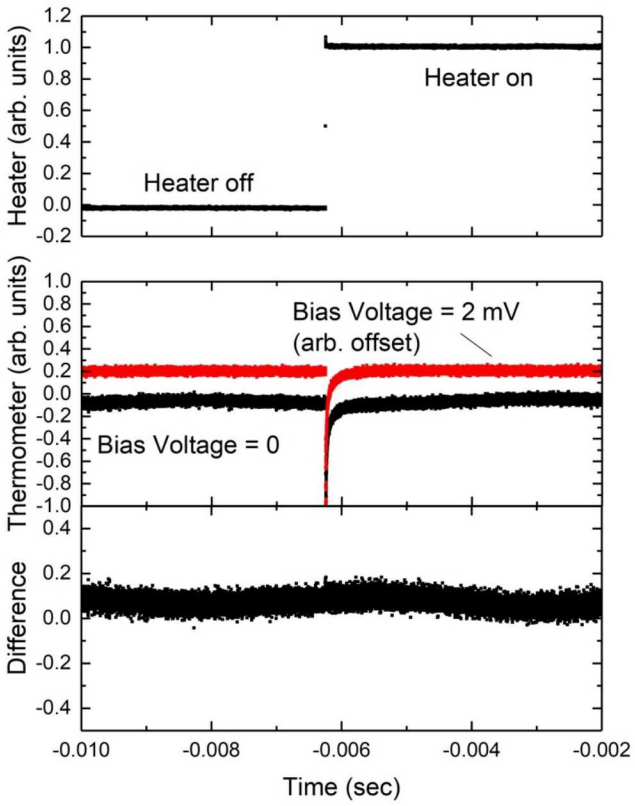


**Fig. 4**. Example measurement of the thermal time constant.

The final step in the measurement is to measure the time constant as the temperature increases on the platform. The time constant is the product of the thermal conductance, which was measured in Fig. 3, and the heat capacity. Thus, a time constant measurement yields the heat capacity. Figure 4 shows an example time trace of the heater output (top panel) and the thermometer signal (middle panel) with two different dc voltage bias points as heater is turned on and off (indicated in the top panel). The signal for each of these measurements is amplified using a variable gain FEMTO trans impedance amplifier with a 1 MHz cutoff frequency. These amplifiers were needed to achieve higher bandwidth than the DL1211 used earlier. The signals were further averaged 1024 time to improve the signal to noise ratio.

## DISCUSSION:

In this system, the time constant is expected to be a millisecond or less at these temperatures. Therefore, one must increase the bandwidth, with a corresponding increase in noise, to accurately measure the thermal time constant. There is a tradeoff between bandwidth and noise. If the noise is too high the small fractional rise in temperature cannot be measured accurately enough to get a good estimate of the time constant. One must inspect the change in thermometer

signal on short time scales as the heater is turned on and off. As shown in Fig. 4, The heater (the top panel shows the output current) is periodically turned on and off. A pulse of 5 ms with a frequency of 80 Hz was applied to the heater at a voltage of 25 mV. The thermometer (middle panel) is then read out as a function of time. The thermometer can be biased with different currents. When the current is zero, no signal is expected from heating. The signature of heating will be larger if there is a larger thermometer current. The red curve corresponds to a voltage bias of 2 mV. The black curve is with the current off. The traces were averaged for 1024 times to improve the signal to noise. The sharp rise and fall at the location of the heater pulse is an electrical artifact of the system, and can be removed by subtracting the two curves. The subtraction is performed in the lower panel. The feedthrough signal has been successfully removed. However, there is no signature of platform heating. The fractional change in current estimated from the thermal conductance and the temperature coefficient of resistance cannot be observed given the large noise floor.

The sharp rise and fall in the signal near the middle of the time trace arises from capacitive coupling somewhere in the measurement circuit and is not thermal in origin. When the voltage bias on the thermometer is zero, there should be no signal arising from heating. When the voltage bias is turned on, heating effects should be present. The two different signals (red and black in the middle panel) have the same feedthrough signal, which can then be subtracted out. This subtraction is shown in the lower panel of Fig. 4. The feedthrough signal is essentially removed from this plot. However, the noise was too high to observe the small expected fractional change in temperature rise. However, this plot allows a noise measurement of the system, enabling of a prediction of what is needed to obtain high fidelity time constant measurements.

Given the data in Fig. 4, which were taken with a 1 MHz bandwidth imposed through the transimpedance amplifiers and accounting for 1024 averages, we observe a noise floor of about 30 pA/sqrt Hz. The time traces were taken over about 10 milliseconds. Given the thermal conductance and temperature coefficient of resistance of the Pt trace, we expect a temperature rise of about 4 K given the pulse voltage on the heater and a change in resistance of about 24 Ohms. This translated to a change in current of about 10 pA, which is well below the noise floor. Assuming a SNR of 10 is needed, we would need to either raise the current bias on the thermometer to unacceptable high values, leading to heating of the platform by over 50 K, use an unacceptably long averaging time (more than 1 billion traces would need to be averaged), reduce the noise floor in the system, and/or use a thermometer material with a larger temperature coefficient of resistance.

Of these options for improving the SNR, changing the thermometer metal and reducing the noise floor will be required. Low temperature amplification will also probably be important for getting a high fidelity signal. Because this calorimeter has a very small time constant, we must raise the bandwidth, letting more noise into the system, making measurements more difficult.

## ANTICIPATED OUTCOMES AND IMPACTS:

The device fabrication that was developed in the project provides Sandia with a new tool for measuring the thermal properties of materials. The next immediate steps for this research are to revise the thermometry such that we have a much larger temperature coefficient of resistance, particularly at lower temperatures. By increasing the thermometer temperature coefficient of resistance we will have a larger measureable signal and be less prone to noise and the systems noise floor. Allowing data to be acquired much faster. To keep the design and measurement simple, we plan to continue using resistance thermometry, and thus, the most obvious choice for improved thermometry would be to incorporate a compound material that undergoes a metal-insulator transition, e.g., Pt-Ge. Another next step, in terms of measurement improvement, would be to design a sample package for high-frequency measurements to remove the capacitive feedthrough observed during the voltage-pulse testing. We envision this type of package having mini-SMP type connectors to receive the coaxially lines and with waveguides mounted on the sample package to confine the electric field, such that spurious capacitive signals may be nearly omitted from the measurement. Moving forward, specific care will be taken to determine which entity in the measurement system sets the noise floor such that we can improve the signal to noise of the system. We will also address the DC offsets observed in the amplifier chain. As we move forward with the next series of measurements, another topic to consider is the shield grounding scheme. For this current work, all coaxial shields were grounded to the cryostat, using a thermally sunk copper bobbin. These measures were taken because of the anticipated need of a >10MHz bandwidth. However, the thermal relaxation of this device is many time slower than expected, and thus, stainless steel coax may be used (which has a much lower bandwidth, relative to copper coax), along with a grounding point that is not the cryostat coldfinger. This relocation of the grounding point may indeed reduce the system noise that could be emanating from the dry system's compressor.

As a successful demonstration of fabricating this calorimeter, we have received verbal confirmation that we will receive a small quantity of follow-on funding to continue this work. This funding will come from a current LDRD project that is beginning its second year with a focus on reversible, adiabatic computing. This funding would be used to integrate superconducting logic devices onto the calorimeter platform and to measure their energy dissipation. The PI of this project has also stated that they will ask for a "plus-up" to get an additional sum of funds for us to target this particular topic. Furthermore, along the lines of continued funding for this research, one of the team members will be submitting a full LDRD idea focused on thermal dissipation in future computing architectures, where the work performed in this project, including the device developed therein, would form the foundation of this proposed work.

An anticipated outcome from this work is the publication of a high-impact journal publication. After implementing the device and the measurement refinements listed at the beginning of this section, we foresee the demonstration of this device and its capabilities being published in a high quality, peer-reviewed journal. A demonstration of this device's sensing capabilities with a thermal payload will be the first manuscript. However, we foresee a series of publications arising from this initial project, where a variety of materials may be studying with this calorimeter, where each material study results in a high-impact publication.

As a tool for performing thermal physics, we anticipate this device being a high-demand CINT user tool and capability. The drive for studying quantum materials, specifically 2-D van der Waals materials, has increased substantially over the last several years. We expect that the calorimeter developed in this project will function as a thermal platform for studying many-body effects in novel 2-D materials. For this approach one can use a drop-casting technique to load material onto the platform or even pattern the material directly onto the central mass and have it be fabricated along with the device itself. In this mode of operation one can seek-out superconducting topological materials, where the onset of superconductivity is revealed by a specific temperature signature in the temperature-dependent specific heat. This same platform can be used to count phonon modes in low dimensional structures. Again, by depositing materials such as nanoparticles (0-D), nanotubes and nanowires (1-D), or flakes (2-D) onto the platform, one can study phonon modes in these systems to better understand lattice waves in low-dimensional systems to better understand quantum size effects.

## CONCLUSION:

In this project we developed a micro/nanoscale calorimeter, including the development of a measurement technique for examining the device's heat capacity as a function of temperature. An outstanding component of this work was the successful development and implementation of the device process flow. For the process flow to be successful, we overcame several technical issues. For example, the silicon nitride stress is stratified, and it transitions from a thicker, average tensile stressed film to a thinner, compressively stressed film. Along this effort, we examined the chemistry of the film growth and studied the initial nucleation process of the film. To combat the compressive nature of this thinner film, we derived new recipes for the deposition process. To mitigate pinhole defects in the nitride film, we developed new processing protocols to protect the top-side nitride film that ultimately forms the membrane structure. The nitride membranes that form the calorimeter are relatively small (~10μm x ~10μm), and the silicon wafers that form the foundation of the process can vary in their thickness by several percent. Because of the significant sensitivity between the wafer thickness and the membrane etch opening, including unwanted artifacts such as crystal plane misalignment and the finite etching of the [111] plane, numerous lithography tests were conducted to home-in on the correct size to form the nitride etch window such that we obtained the desired membrane size.

Measurements of the microfabricated calorimeter were performed in a closed-system cryostat, where, after a low-level electrical calibration of the thermometer, we used resistance thermometry to determine the temperature rise of the calorimeter plate during an applied heating pulse. From room temperature to around 15K, both the heater and the thermometer exhibited a temperature coefficient of resistance of the order $\sim 10^{-3} K^{-1}$. The calibration of the thermometer was done using a standard lock-in amplifier. We attempted to measure the RC thermal time constant of the platform by apply a voltage pulse to the heater, while DC voltage biasing the thermometer. Due to capacitive feedthrough and the low level of current change that was to be observed in the thermometer during a heating event, appreciable heating was required to observe

any significant change in the thermometer's temperature. This heating could be on the order of ~10K. The back ground electrical capacitance signal can be effectively subtracted from the signal of interest, such that one can observe the transient response of the platform during a heating event. However, DC offsets in the amplifier chain can still produce spurious signal changes and must be accounted for by the nulling of these signals. If these offsets remain, then the steady-state response of the thermometer will not provide a true measure of the platforms intrinsic thermal resistance. Alternative methods to determine the calorimeter's thermal resistance include using a DC source to drive the heater and using a lock-in amplifier to measure the temperature response of the thermometer. When combined with the TCR from the calibration measurement, we observed a total thermal resistance of ~$10^8$ K/W at 300K. From scope traces, we see a transient response of approximately 1ms. Combining the thermal resistance and time constant, we estimate the calorimeter's heat capacity to be approximately ~$10^{-11}$ J/K at room temperature.

## REFERENCES:

1. M. Zhang, M. Yu. Efremov, F. Schiettekatte, E. A. Olson, A. T. Kwan, S. L. Lai, T. Wisleder, J. E. Greene, , and L. H. Allen. Size-dependent melting point depression of nanostructures: Nanocalorimetric measurements. *Phys. Rev. B*, **62**(15):10548–10557, 2000.

2. J. Hone, B. Batlogg, Z. Benes, A. T. Johnson, and J. E. Fischer. Quantized phonon spectrum of single-wall carbon nanotubes. *Science*, **289**:1730–1733, 2000.

3. P. F. Sullivan and G. Seigel. Steady-state, ac-temperature calorimetry. *Phys. Rev.*, **173**(3):679–685, 1968.

4. M. L. Roukes. Yoctocalorimetry: phonon counting in nanostructures. *Physica B*, **263–264**:1–15, 1999.

5. G. R. Stewart. Measurement of low-temperature specific heat. *Rev. Sci. Instr.*, **54**(1):1–10, 1983.